

Diffusive Dynamics of the Reaction Coordinate for Protein Folding Funnel

N. D. SOCCI AND J. N. ONUCHIC

Department of Physics-0319, University of California at San Diego, La Jolla, California 92093

P. G. WOLYNES

School of Chemical Sciences, University of Illinois, Urbana, Illinois 61801

In press: *J. Chem. Phys.*, April 15, 1996

ABSTRACT The quantitative description of model protein folding kinetics using a diffusive collective reaction coordinate is examined. Direct folding kinetics, diffusional coefficients and free energy profiles are determined from Monte Carlo simulations of a 27-mer, 3 letter code lattice model, which corresponds roughly to a small helical protein. Analytic folding calculations, using simple diffusive rate theory, agree extremely well with the full simulation results. Folding in this system is best seen as a diffusive, funnel-like process.

I Introduction

Protein folding is a collective self-organization process, conventionally described as a chemical reaction. However, this process generally does not occur by an obligate series of discrete intermediates, a “pathway,” but by a multiplicity of routes down a folding funnel.¹⁻⁷ Dynamics within a folding funnel involves the progressive formation of an ensemble of partially ordered structures, which is transiently impeded in its flow toward the folded structure by trapping in local minima on the energy landscape. As one proceeds down the folding funnel, the different ensembles of partially ordered structures can be conveniently described by one or more collective reaction coordinates or order parameters. Thermodynamically this funnel is characterized by a free energy that is a function of the reaction coordinate which is determined by the competition between the energy and entropy. A crucial feature of the funnel description is the concerted change in both the energy and the entropy as one moves along the reaction coordinate. As the entropy

decreases so does the energy. The gradient of the free energy determines the average drift up or down the funnel. Superimposed on this drift is a stochastic motion whose statistics depends on the jumps between local minima. To first approximation this process can be described as diffusion. Folding rates are determined both by the free energy profile of the funnel and the stochastic dynamics of the reaction coordinates. In this paper we study the dynamics of a reaction coordinate describing the folding funnel of a lattice model with thermodynamic parameters which theoretical arguments suggest realistically correspond with fast folding small helical proteins.³ We determine from simulation both the free energy profiles and effective configurational diffusion coefficients for a folding reaction coordinate as a function of temperature. Folding times, also determined by simulations, are compared to analytical calculations based on these quantities.

The kinetic analysis of a single folding funnel is most appropriate for the fast folding proteins that mainly flow downhill progressively in energy to the folded state. During folding, even for this case, trapping in local minima will occur for times very short compared the overall folding time. Alternatively, when the residence time in these traps becomes too long leading to a substantial slow down of the folding time, the traps can be thought of as creating additional funnels. This occurs near the glass transition of the heteropolymer. Good folding sequences will fold at a temperature T_f , which is above the glass transition temperature, T_g , and have a single dominant folding funnel. As the chain moves downhill energetically in its dominant funnel and becomes more similar

to the native structure, the configurational entropy of the chain (number of available states) is reduced. For the model discussed here, a single order parameter suffices to measure similarity. For real proteins more order parameters may be necessary to quantify the similarity of the configuration to the native structure for example: degree of collapse, helicity as well as fraction of correct contacts and dihedral angles in the general case. A free energy surface as a function of these order parameters can then be calculated. For the case of a single dominant funnel, these order parameters may also be associated with reaction coordinates. The motion of these reaction coordinates will be largely diffusive due to the transient trapping. For the single funnel case, the folding time is generally determined both by the difficulty to overcome the free energy barrier and a prefactor that depends on the ruggedness of the landscape that enters via the diffusion coefficients. This general quantitative description of folding using diffusive coordinates along with energy landscape ideas to account for trapping was introduced by Bryngelson and Wolynes^{8,9} (BW). A short overview of their ideas is given in the next section. Many of the qualitative ideas from that description (e.g. the importance of the relationship between T_f and T_g for kinetics) have been qualitatively confirmed in lattice studies of model proteins^{10,11} and others have studied the dynamical properties of these model systems.^{6,12-15} The main goal of the present paper is to quantitatively compare the BW expressions for the folding time and effective diffusion coefficients with the simulation results over a range of thermodynamics conditions for a model that theory suggests realistically corresponds with the faster folding small proteins.

In a previous paper,³ we started this analysis. There it was shown that at the folding temperature (T_f) the trajectories of appropriate collective reaction coordinates are Brownian and must surmount a modest thermodynamic free energy barrier. The folding time at T_f was well described by the diffusive rate formula. This work shows how, using a combination of simulation results and analytical theories, to formulate a law of corresponding states relating simple lattice models to small helical proteins. Since free energy surfaces are temperature dependent, various scenarios for the folding mechanism apply at different temperatures.² By testing the validity of analytical formulas over a wide temperature range, we hope to provide a route to use theoretical descriptions to design and understand quantitative experiments.

II A summary of the Bryngelson and Wolynes Energy Landscape Picture

The energy landscape of any heteropolymer is complex. Because of the possibility of making many contacts involving residues that are distant in sequence, the energy landscape is rough. This is an effect of frustration. Protein-like heteropolymers obey a principle of minimal frustration, leading to an additional funnel-like aspect of the landscape. To quantify this, we recognize that the energy landscape is stratified, that is to say the statistical characteristics of the landscape depend on the distance from, or equivalently the similarity to, the ideal native structure. This similarity measure is known as an order parameter in the physics of phase transitions, and for small systems such as proteins can also be used as a reaction coordinate for computing the folding rate. (Here this the reaction coordinate will be called n .) Clearly such a reaction coordinate is not unique. A picture of such a stratified landscape with kinetic connections is shown in figure 1. BW show that to a first approximation, the folding time can be computed by first grouping together states with in a stratum having a common value of the reaction coordinate. A diffusion equation for the probability flow between strata is derived under the assumption that the reaction coordinate can only change by relatively small steps, and it is written as

$$\frac{\partial P(n,t)}{\partial t} = \frac{\partial}{\partial n} \left\{ D(n) \left[\frac{\partial P(n,t)}{\partial n} + P(n,t) \frac{\partial \beta F(n)}{\partial n} \right] \right\} \quad (1)$$

The average direction of the flow is given by the gradient of the free energy. The diffusion coefficient, $D(n)$, depends on the trapping in local minima and reflects the ruggedness of the energy landscape in the system proximity of the glass transition.

The free energy $F(n)$ incorporates the balance between two terms, the energy that is decreased as the native state is approached and the entropic term $-TS(n)$ which decreases with unfolding. The shape of the free energy profile is therefore strongly temperature dependent as illustrated in figure 1b. At high temperatures, folding is an uphill process thermodynamically so folding is exponentially suppressed. At the folding temperature, the free energy profile is typically bistable with a small thermodynamic barrier which arises from the incomplete cancellation of the entropy by the energy as the systems descends through the funnel. At low temperatures, folding becomes a downhill process. Thus, if the diffusion coefficient were temperature independent, the rate of

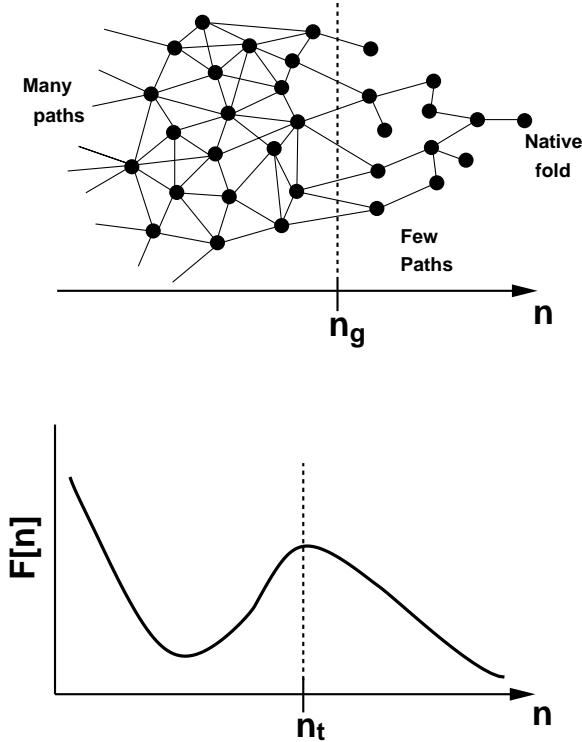


Figure 1: The top figure shows the kinetic landscape versus an arbitrary reaction coordinate (n). The vertical line shows the glass transition point (n_g) in which the behavior changes from many paths to few paths. In addition to the native state there are a number of local minimum. The bottom figure shows the free energy plotted as a function of the same coordinate. The line at n_t denotes the transition region.

folding would have a dependence on the thermodynamic driving force (which depends on $1/T$) just as a solid state rectifier depends on the applied voltage (as in the famous example of Feynman). The folding time can be written as a double integral

$$\tau_f = \int_{n_{\text{unf}}}^{n_{\text{fold}}} dn \int_0^n dn' \frac{\exp[\beta F(n) - \beta F(n')]}{D(n)} \quad (2)$$

When the barrier exists, as at T_f , $F(n)$ has a double-well with the bottom of one well close to n_{unf} and the bottom of the other well at n_{fold} . In this situation this double integral can be approximated by a Kramer's like law,^{16,17}

$$\tau_f = \left(\frac{2\pi}{\beta}\right)^{1/2} \frac{\exp\{\beta [\bar{F}(n_t) - F(n_{\text{unf}})]\}}{D_0 \omega_{\text{unf}} \bar{\omega}_{\text{fold}}} \quad (3)$$

where

$$\bar{F}(n) = F(n) - TX(n) \quad (4)$$

and

$$X(n) = \log \left[\frac{D(n)}{D_0} \right], \quad (5)$$

and ω_{unf} is the curvature around n_{unf} and $\bar{\omega}_{\text{fold}}$ is the curvature in the top of the barrier. D_0 is the effective diffusion coefficient on an equivalent flat landscape.

The prefactor of Kramer's expression reflects the multiple recrossings of the barrier through diffusion that is controlled by trapping. When the process is entirely downhill, the double integral becomes simply proportional to the diffusion coefficient, and only weakly depends on the slope of the free energy gradient.

The configurational diffusion coefficient depends both on the local moves allowed to the protein and the energy landscape topography. BW analyzes configurational diffusion by assuming the limit of an uncorrelated rugged energy landscape and Metropolis rules. This is, of course, a caricature of the dynamics in which the landscape will have correlations and the barriers to escape from traps may be surmounted by successively melting out local clusters rather than globally changing the protein conformation. According to the BW analysis, the diffusion coefficient has a strong temperature dependence that arises from the necessity to escape from local minima on the rough energy landscape. At high temperatures, D follows a Ferry law typical of glasses,

$$D(T, n) = D_0 \exp[-\beta^2 \Delta E^2(n)] \quad (6)$$

where $\Delta E^2(n)$ is the local mean square fluctuation in energy. At intermediate temperatures, the strongly non-Arrhenius temperature dependence becomes itself moderated

$$D(T, n) = D_0 \exp\{-S^*(n) + [\beta_g(n) - \beta]^2 \Delta E^2(n)\} \quad (7)$$

This equation is valid for temperatures between $T_g(n)$ and $2T_g(n)$. This form arises because of the assumed Metropolis dynamics. The characteristic temperature is the ideal glass transition where the configurational entropy would vanish at equilibrium. This is given by the condition

$$T_g(n) = \frac{\Delta E(n)}{[2S^*(n)]^{1/2}}, \quad (8)$$

where $S^*(n)$ is configurational entropy at n . We see that at T_g , the diffusion coefficient is diminished from its bare value by a factor of the total number configuration states, thus giving rise to a possibility of a Levinthal paradox. Below T_g , we expect both that

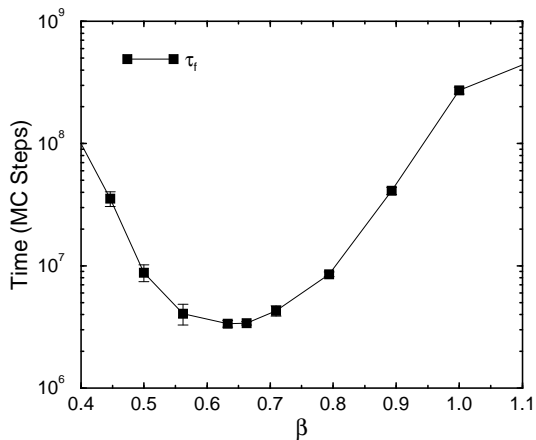


Figure 2: Mean first passage time (τ_f) is plotted as a function of the inverse temperature (β). Note, parabolic dependence of the folding time on β .

the diffusion coefficient will still possess an activation energy but the activation energy will not be self-averaging and that the free energy itself can fluctuate considerably and will be very sensitive to details of the model and to the sequence of the heteropolymer. In the theory of disordered systems this is known as the emergence of non self-averaging behavior, the hallmark of the ideal thermodynamic spin glass transition in mesoscopic systems. Below T_g , the slow folding process can be better described by a few kinetic pathways than by the statistical average laws appropriate for the faster events. Both the temperature dependence of D and the interplay of entropy and energetic ruggedness in the driving force lead to a parabolic dependence of the folding rate on the inverse temperature as shown in figure 2. This rough form has been confirmed in many lattice simulations. Leite and Onuchic¹⁸ have shown that for an energy landscape model for solvent polarization, analogous to the BW landscape, there is a gradual transition into a slow non-self averaging dynamics. Fluctuations gradually dominates the kinetics below this temperature.

Folding rates depends on both diffusion and free energy profile in a way that is significantly different from the standard transition state theory (TST) The extent to which the rate is determined by the free energy profile versus the diffusion coefficient, that incorporates the multiple barrier crossing, depends on the choice for the reaction coordinate. Notice however, that while it may be impossible or at least difficult to find a reaction coordinate for which TST is exact, the diffusion formula (eq. 2) is essentially invariant

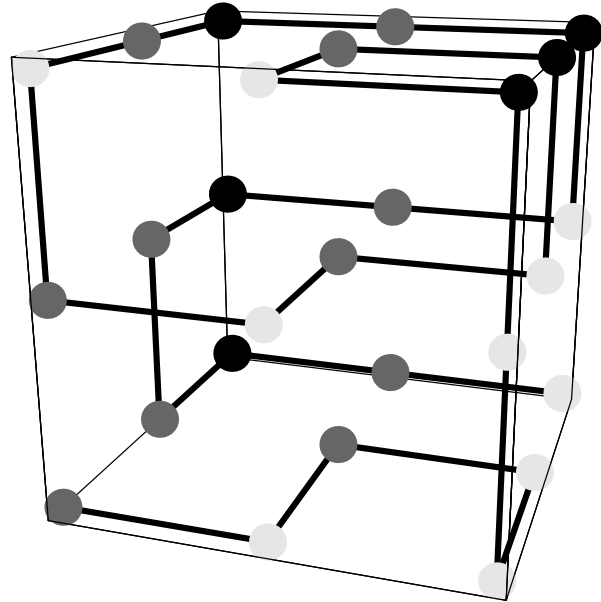


Figure 3: The native state (minimum energy) cube for the sequence studied in this work. The sequence (ABABBBACBACBABABACACBACAACAB) consist of three monomer types.

to this choice as long as the elementary moves are reasonably local for this coordinate.

In the original BW treatment, this reaction coordinate was represented by an order parameter ρ that measured the similarity between any given configuration and the native state of the protein in terms of the fraction of correct dihedral angles, a coordinate which is manifestly local because of the elementary moves of the protein at the microscopic level are controlled by isomerization of the peptide bond. Another possible reaction coordinate is the number of correct contacts, a coordinate that is only partially local.

III Configurational diffusion for lattice models in proteins

Are these general ideas developed by Bryngelson and Wolynes (BW) valid for quantitatively predicting folding times in model proteins with a realistic energy landscape topography? We show in this section that as long as the glass transition falls after the transition region (top of the barrier in the free energy profile for the collective reaction coordinate) that this is the case. In this limit the single dominant funnel picture is appropriate. The system under study is the designed three-letter code 27-mer lattice model (see figure 3) used in our recent studies.^{3, 10, 11} Although this 27-mer is far from being a real protein, it has

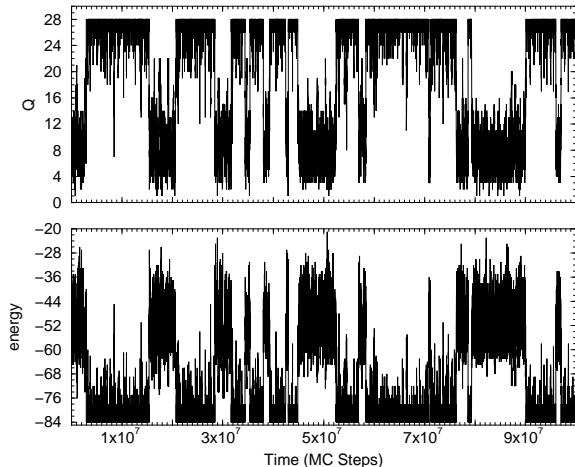


Figure 4: The energy and order parameter (Q , the number of *correct* native contacts) plotted as a function of time for a sample folding simulation. The temperature is the folding temperature ($T_f = 1.51$). The time is roughly 30 times the folding time ($\tau_f \approx 3 \times 10^6$). The plot shows the two-state-like behavior of this system with transition between the native state ($E = -84$, $Q = 28$) and a molten globule region ($E \approx 50$, $Q \approx 7$). The transition are extremely rapid with respect to the folding time. In addition there are significant fluctuations about the two states.

been shown³ that by developing a law of corresponding states, the results obtained for such a system can be used to describe a small α -helical protein. In these simulations the units of temperature and energy are such that $k_b = 1$. This still leaves an arbitrary scale factor since the only important quantity is the ratio of energy to temperature. We have chosen small, integer values for the coupling energies for convenience and efficiency. The kinetic glass temperature is $T_g \sim 1$.

Figure 4 shows the time evolution at T_f for energy and the Q order parameter. This Q parameter is a measure of similarity to the native state and is equal to the number of *correct* contacts (i.e. contacts that exist in the native state). It ranges from 0, no correct contacts, to 28, the maximum number of possible contacts. Figure 5 plots the energy, entropy and free energy as a function of Q for various temperatures. At temperatures above the glass temperature, there is a significant gradient in both energy and entropy. These profiles are computed from the density of states obtained using the Monte Carlo histogram technique.¹¹ Starting from a random configuration, collapse occurs at times very short compared to the folding time. Thus in this parameter range, the radius of gyration need not be considered as a separate dynamical reaction coordinate; however, in

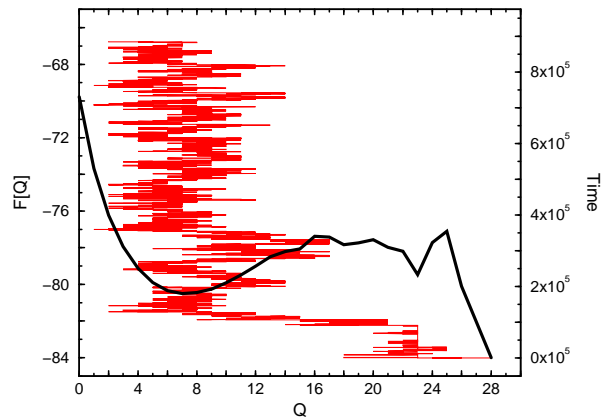


Figure 6: A folding trajectory ($Q(\tau)$) superimposed on the free energy ($F[Q]$) at the folding temperature. The trajectory is approximately 9×10^5 Monte Carlo steps long (approximately 27% of τ_f). The right axis shows the time counted backwards from the folded state. Note, most of the time is spent diffusing in the molten globule region. Once the barrier is surmounted folding proceeds rapidly. Numerous recrossings of the barrier region indicate the need to use a diffusive theory for this reaction coordinate not transition state theory.

determining the free energies one must note that the mean radius of gyration does vary with temperature. A molten globule band, where configurations have an average of 20 contacts and $Q = 7.5$ ($\approx 27\%$ similarity to the native state), describes the region where this sequence spends most of its time on its way into the folded state. The shape of the free energy in the vicinity of this mean Q is quasi-harmonic, although in fact large deviations are possible at high temperatures. As shown in our earlier work, since at T_f the local glass transition as a function of Q occurs after the transition region has been overcome, the folding time is determined primarily by the time taken to overcome the free energy barrier, i.e., to cross the transition region. Figure 6 shows a folding trajectory of the Q coordinate superimposed on a plot of the free energy. The plot shows a time span which is roughly one quarter of the mean folding time (τ_f) at this temperature. Most of the trajectory consists of diffusive motion about the molten globule region. Once the barrier has been surmounted folding occurs rapidly, taking roughly 10^5 Monte Carlo steps ($\approx .03\tau_f$).

However, to estimate the folding times at a variety of temperatures, knowledge of the free energy barrier alone is not sufficient. Information about the dynamics must be obtained by calculating the con-

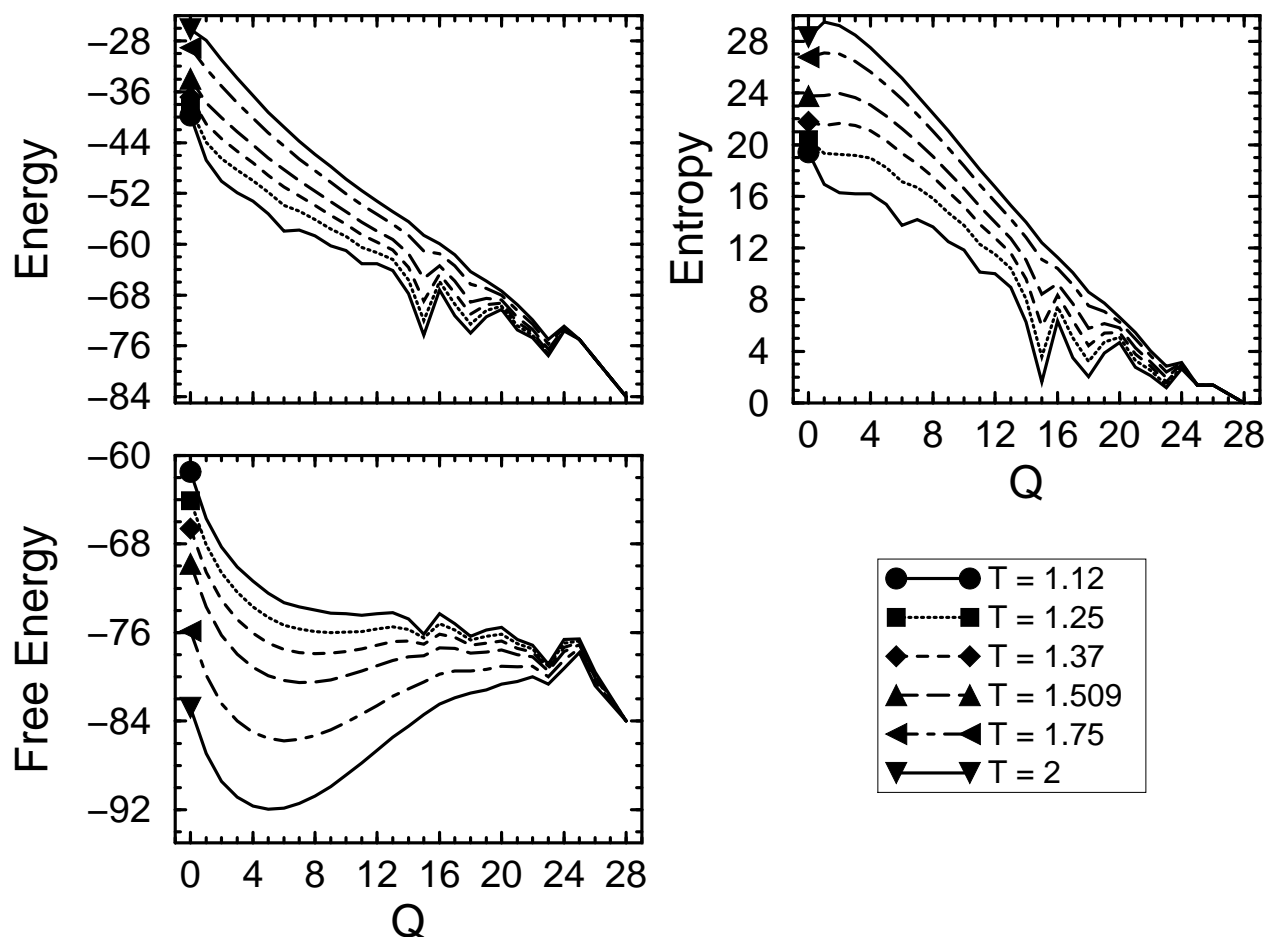


Figure 5: Energy, entropy and free energy as a function of Q for several temperatures calculated using the Monte Carlo histogram method.¹¹ For a broad range of temperatures the free energy has a clear double well form: one at the native state ($Q = 28$) and one at the molten globule region ($Q \approx 7$). The double well form is consistent with the two state behavior scene in figure 4. Above the glass transition temperature ($T_g \sim 1$) there is a significant energy and entropy gradient between the molten globule region and the transition region ($Q \approx 15$). Both ΔE and ΔS are less than zero, so the unfavorable reduction in entropy is offset by a loss in energy, leaving a small free energy barrier at the folding temperature ($T = 1.509$). As the temperature approaches the glass temperature the energy and entropy gradients decrease as does the free energy barrier. However the folding time diverges due to the increase in the diffusion constant of the system (i.e., the roughness of the energy landscape).

figurational diffusion coefficient through the complex energy landscape. As described in the previous section, when a single reaction coordinate is considered, for example Q , τ_f can be computed using the double integral give by eq. 2. In general the diffusion coefficient will depend on Q but, one more simplification is assumed here. Only the average value of D , computed for states in the molten globule band, is inferred from simulations. We do this by computing the correlation function of the fluctuations of the reaction coordinate $\Delta Q(t)$. Within the quasi-harmonic diffusive approximation this correlation function should decay exponentially at long times. The configurational diffusion coefficient will be related to the corresponding correlation time and the mean square instantaneous value of the reaction coordinate fluctuations, $\Delta Q^2(T)$. (This calculation is constrained for values of Q before the transition region.) At a given temperature, the diffusive harmonic model gives $D = \Delta Q^2(T)/\tau_{\text{corr}}(T)$. Since $\tau_{\text{corr}} < \tau_f$, it is a quantity that is much easier to obtain from numerical simulations for more complex systems such as atomistic simulations of proteins. For experimentalists we especially wish to point out this viewpoint and the corresponding approximation allow one to use dynamic probes of fluctuations in the molten globule state at equilibrium to predict the rate of the non-equilibrium folding process.

In figure 7 we show the simulated τ_{corr} and diffusion coefficient for various temperatures above the glass transition. The autocorrelation time as been calculated in the molten globule region. To do this, the correlation function $\langle Q(t)Q(0) \rangle$ was calculated over paths which were confined to the molten globule region of the conformation space. For these calculations we define any conformation with $Q < 17$ as being in the molten globule region. The decays are in fact non-exponential for short times. We have not analyzed the non-exponentiality in detail. The information would provide the dynamics of individual conformation steps and should contain information on the distribution of substate lifetimes. We identify the long time decay with the effective diffusive harmonic value. A more complete model should account for this short time decay via a frequency dependent diffusion coefficient as proposed by BW. Frequency effects may be important for determining the prefactor of barrier crossing as discussed by Grote and Hynes for simple chemical reactions.¹⁹

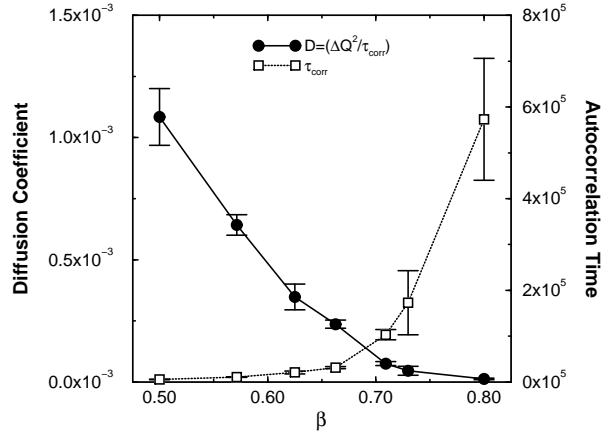


Figure 7: Autocorrelation time (τ_{corr}) and diffusion coefficient ($\Delta Q^2/\tau_{\text{corr}}$) plotted as a function of the inverse temperature (β). At low temperature (high β) the diffusion coefficient decreases rapidly while the correlation time increases, indicating a slow down of the dynamics due to trapping in local minimum.

IV Details of simulations and comparison with BW analysis

To study the dynamics of this model we used the Monte Carlo algorithm with local moves, which include end moves, corner flips and 90° crankshaft moves. The excluded volume constraint was enforced by not allowing any multiple occupancy. (Further details can be found in a previous work.¹⁰) To calculate the mean first passage time (τ_f) as a function of temperature the following procedure was used. For each temperature many simulations were performed, each starting from a different random unfolded initial condition. The simulations were run until the chain found the folded state or until a maximum number of time steps τ_{max} had elapsed. The mean first passage time is simply the average of the folding times for the different runs. For an intermediate range of temperatures all of the runs would find the folded state within τ_{max} steps. However for very low and high temperatures only some fraction would find the folded state in the allowed time. For these temperatures the mean calculated is a *lower bound* to the actual mean first passage time. This is because for trials that do not fold within τ_{max} steps, we average in τ_{max} which is less than the actually folding time for that run. This is done for practical reasons since we have a finite amount of computer time for the simulations. The key point is that τ_{max} is much greater than τ_f for a broad range of temperatures; which in fact, it is. Figure 2 shows the mean first passage time

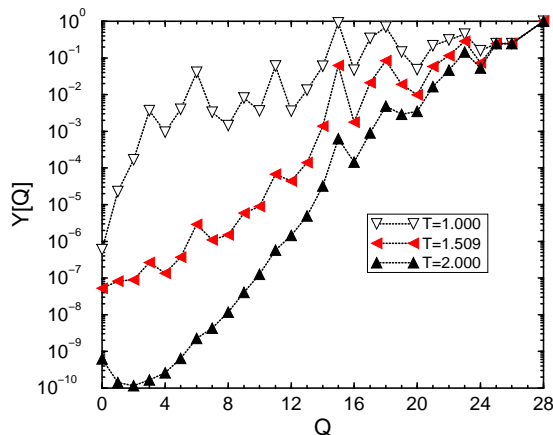


Figure 8: Qualitative replica symmetry breaking value $Y(Q) = \sum_i [P_i(Q)]^2$ plot at three temperatures (T_g , T_f and $2T_g$). Note that although at the global glass temperature (T_g) discrete states are apparent even for small degrees of nativeness, at the folding temperature the discrete intermediates are largely native-like.

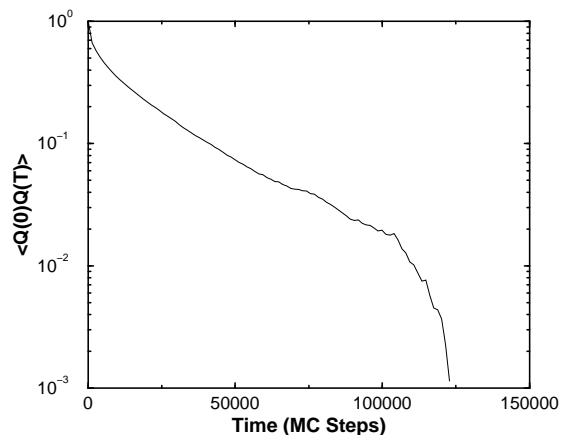


Figure 9: Autocorrelation function for Q (see eq. 9) plotted on a semi-log scale. $T = T_f$. The correlations have an initial rapid decay followed by a slower decay. By fitting a sum of exponentials (usually 3 or 4) the autocorrelation time can be determined.

simulated for a range of temperatures.

At low temperatures, τ_f grows rapidly. This slow down is caused by trapping in local minima. It is well known that heteropolymers undergo an ideal glass transition at low enough temperature. The random energy model estimate of this temperature for the present system is $T_g^{REM} = \Delta E^2 / \sqrt{2S_L}$. The measured energetic fluctuations ΔE^2 's are 51 at τ_f and 22 at $T = 1.1$ (slightly above the glass transition). The respective configurational entropies for the collapsed states, S_L , are around 20 and 12. Both cases provide a $T_g^{REM} \sim 1.0$. This agrees with the critical temperature at which replica symmetry breaking sets in. This is determined by finding the temperature at which $Y = \sum_i P_i^2$ becomes of order 1 (see figure 8). P_i is the Boltzmann occupation of a microstate. Y is not the perfect measure of replica symmetry breaking since it assumes the basin of attraction of a microstate can be identified with the state itself. The corresponding neglect of correlation between these high Q states, however, is able to provide a reasonable estimate of T_g for a finite mesoscopic system.

These estimates of T_g are very similar to those of the *kinetic glass transition* which is the temperature at which the folding time slows down substantially. We define the kinetic glass transition temperature (T_g) to be the temperature at which the folding time is sufficiently slower than the fastest folding time observed. There are several ways of choosing this point which will give roughly the same answer. We choose

T_g , to be the temperature at which $\tau_f = \frac{1}{2}\tau_{\max}$. For this sequence, $T_g \approx 1$.

In addition to the kinetic runs to calculate τ_f , we performed a number of thermodynamic runs to determine the free energy profiles. Again most of the details can be found in a previous work.¹¹ We used the Monte Carlo histogram technique which allows us to calculate extensive quantities like the free energy. The basic idea is to store a histogram as a function of Q and E . These histograms measure the probability that a given (Q, E) pair will occur. From these we can calculate the density of states $n(Q, E)$ up to a multiplicative constant (which can be determined since we know the $n(1, E_{\min}) = 1$). We can then calculate any thermodynamic quantity; in particular, we determined the free energy as a function of Q ($F[Q]$) for several temperatures. The free energy is shown in figure 5. For a broad range of temperatures the free energy has a rough double well profile, with one minimum at the folded state ($Q = 28$) and another for the molten globule ($Q \approx 5-7$). The transition state varies from $Q^\ddagger = 22$ at $T = 2$ to $Q^\ddagger = 16$ at the lower temperatures. At first it might appear the transition state is at $Q^\ddagger = 25$ since this is the highest local maximum in the plot at most temperatures.²⁰ However, this turns out not to be the correct transition point. One must be careful in interpreting free energy plots of this type. There are Monte Carlo moves that connect states with $Q = 23$ directly to the ground state short circuiting this barrier. In fact any barrier that is smaller in width than 5 can also

be by passed by certain Monte Carlo moves. Note, the correct barriers from 22 to 16 are much broader. In fact it is better to think in terms of a transition “region” rather than a unique transition point. The way in which we identified this region was to look at the time trajectories (figure 4). Since we are in a diffusive regime, a trajectory that reaches the transition region should have some probability of diffusing back down the barrier rather than crossing over. For Q^\ddagger values between 16–22 we see such an effect. However, by the time $Q^\ddagger = 25$ is chosen there would be virtually no trajectories that cross back without first reaching the folded state. We have also previously used a 2 dimensional analysis of the trajectories and free energy surfaces and again we find the transition region to be between 16-22 and not at 25.³ Since we know that the transition state is somewhere between 16 and 22 we define a specific transition point, for use in calculating the barrier for the Kramer’s rate equation, as the value of Q that is a maximum *in this region*.

In addition to the free energy barrier we need to measure the diffusion coefficient in this system in order to calculate the folding time. We compute the diffusion coefficient by measuring the autocorrelation time of Q . Specifically we calculate:

$$C_Q(\Delta) = \frac{\langle Q(t)Q(t+\Delta) \rangle - \langle Q(t) \rangle^2}{\langle Q^2(t) \rangle - \langle Q(t) \rangle^2} \quad (9)$$

Figure 9 shows a semi-log plot of the auto correlation function at $T = 1.509$, the folding temperature. The figure is multi-exponential with a short fast decay followed by a much longer, slower decay. The final drop-off is mostly due to errors in sampling at very long times. We are interested in the long time decay and calculated the exponent associated with this by fitting a function of several exponentials (usually 3 or 4) to this plot. We repeated this calculation at several temperatures (note that we can not use the histogram method here do the large amount of histogram information that would have to be stored). Figure 10 is a log-log plot of the autocorrelation function for several temperatures. As the temperature is decreased the autocorrelation time increases. Finally the diffusion coefficient was estimated as $D = \Delta Q^2 / \tau_{\text{corr}}$.

With the diffusion coefficients and free energy surfaces in hand, it is now possible to test the analytical prediction given by eq. 2. Using the discrete form of the full double integral (with a constant diffusion coefficient):

$$\tau_f = \frac{1}{D_0} \sum_{Q=0}^{23} \sum_{Q'=0}^{Q-1} \exp \{ \beta (F[Q] - F[Q']) \} \quad (10)$$

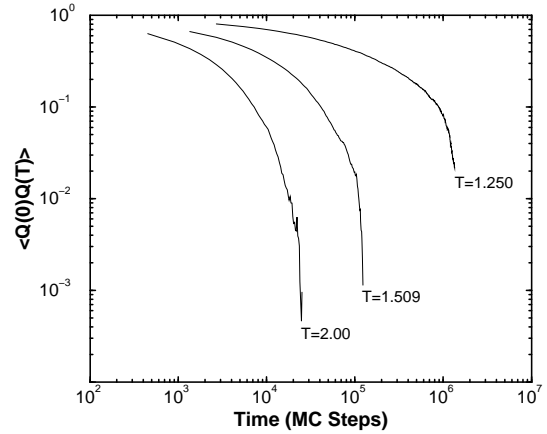


Figure 10: Q Autocorrelation function plotted on a log-log scale for several temperatures. As the temperature decreases the correlation time increases.

we obtain the results presented in figure 11. Note the sum is not taken to $Q = 28$ since we do not expect the diffusion coefficient to remain constant in that region (between $Q = 23$ –28). However, the time it takes to go from $Q = 23$ to the folded state ($Q = 28$) is small compared to τ_f (as seen in figure 6) so the error from truncating the sum will also be small. Overcoming the barrier ($Q \approx 17$) is the limiting step. Additionally, we can also use a simplified form of eq. 2 which assumes that the free energy surface is well approximated by a parabolic potential around the molten globule states that extends all the way to the barrier (eq. 3). If we further assume that $D(n) = D_0$ and that the two curvatures are the same then the folding time is given by $\tau_f = 2\pi\tau_{\text{corr}}e^{\Delta F/T}$ (which is also shown in figure 11). This simple result is useful because it depends only on the correlation time in the molten globule and the free energy barrier. The agreement with the full formula is remarkable. For both formulas, the fastest time at the optimal kinetic folding temperature is obtained to well within a factor of two. Also, an extremely good description of the behavior for the slow down anticipated for low and high temperatures is obtained. Thus we see the analytical theory based on the actual molten globule dynamics and funnel free energy profile is not simply qualitatively correct but can be used for quantitative predictions of the folding time over a wide thermodynamic range.

Up to this point, the values for the diffusion coefficients have been obtained directly from the simulation data for the time correlation functions around the molten globule. It is interesting now to com-

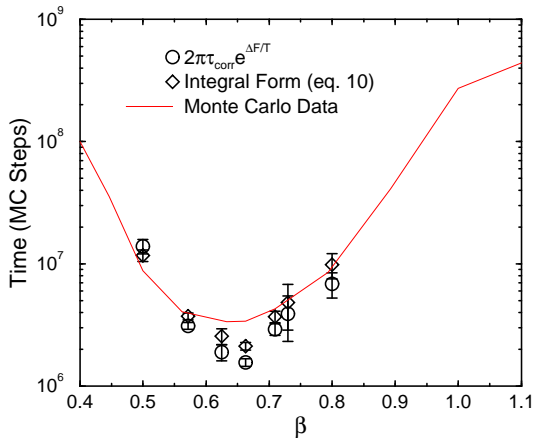


Figure 11: Comparison of mean first passage times from Monte Carlo simulations with folding times calculated both the discrete form of the double integral (eqs. 2 and 10) and the simple rate formula $2\pi\tau_{\text{corr}}e^{\beta\Delta F}$ which assumes a constant diffusion coefficient and that the curvature at the top and bottom of the free energy are the same.

pare the obtained results with the existing models of configurational diffusion, particularly the BW theory. Since our results fall in the range between T_g and $2T_g$, the intermediate temperature formula given by eq. 7 would be seen to be the appropriate comparison. Figure 12 shows a plot of the diffusion coefficients as a function of $(\beta_g - \beta)^2$. The slope obtained from the semi-log plot provides a fitted value for ΔE^2 of ~ 15 . This is a little bit smaller than the ΔE^2 's obtained directly from simulations at this temperature range. This is expected because correlations in the landscape cause only part of the total energetic ruggedness to come into the activation barriers for escaping from traps. Qualitative agreement between the model and simulations suggests that while the *REM* results are a first approximation, the correlations in the energy landscape are significant and the effective fluctuations for escape from a trap involves only a fraction of the chain.^{18,21} We would expect these correlation effects to become more important as the effective chain length of the protein grows, however we should bear in mind that the same qualitative behavior still applies. In the temperature range studied, we note the data could be equally well fitted by an Arrhenius temperature plot (see figure 13). The effective activation energy is ~ 10 ($\sim 7k_B T_f$). This very large number implies that the effective moves of Q require substantial organization of the protein since the stability gap is only $20k_B T_f$. The simple Ferry law fit is also adequate providing a $\Delta E^2 \sim 8$

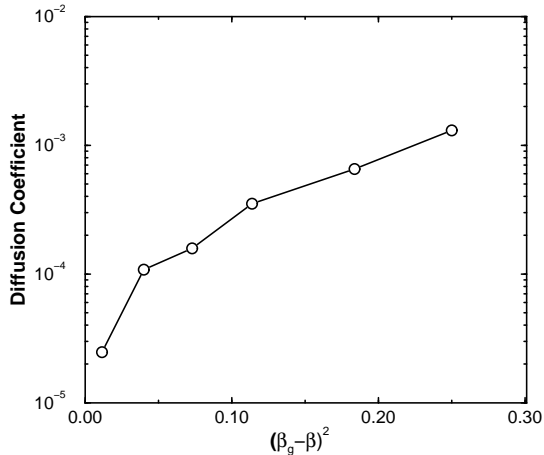


Figure 12: Diffusion coefficient plotted versus $(\beta_g - \beta)^2$

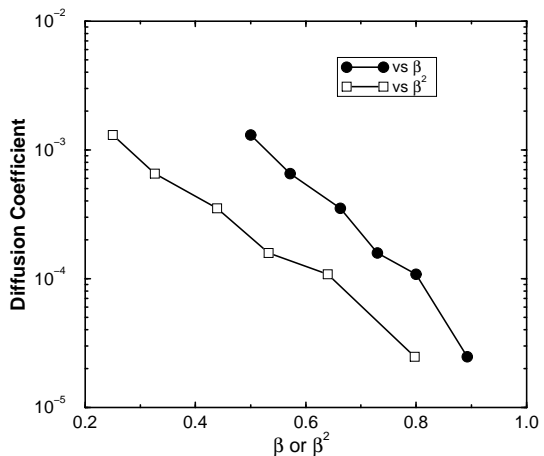


Figure 13: Diffusion coefficient plotted versus β and β^2

(see eq. 4 and figure 13).

V Conclusions

Protein folding is remarkable as a chemical reaction with a highly non-Arrhenius temperature dependence. Although for real proteins some of this behavior is doubtless due to the entropic nature of hydrophobic forces, we see here that this unusual temperature dependence also arises from the competition between trapping in misfolded states and drift down the folding funnel which is itself a competition between entropy and energy. These effects can be described through collective coordinates, which make quantitative the nature of the funnel. Our results establish that a description in terms of a single collective coordinate suffices to explain folding kinetics of small lattice models over a wide range of temperatures. We believe that a similar set of concepts can be used for the smaller real proteins because of their correspondence with the lattice models. The diffusive dynamics should be contrasted to the more traditional transition state theory. These simulations suggest that if transition state theory is used a very complex reaction coordinate, reflecting the detailed trapping dynamics, would have to be constructed. The single collective diffusive coordinate picture on the other hand is much more robust and can make use of experimental information about the dynamics of fluctuations in the molten globule, as well as simple thermodynamic measurements and theories about the molten globule state.

The lattice model studied here are described quite well by a single order parameter or reaction coordinate. Various scenarios for protein folding require the introduction of a few more collective coordinates to describe the funnel. Even the small helical proteins, that corresponding in a thermodynamic sense with the 27-mer lattice, require the introduction of coordinates describing the amount of helicity, degree of collapse and liquid crystallinity of the dynamical molten globules. If these order parameters are constant or their dynamics is “slaved” to the tertiary ordering parameter the one-dimensional diffusive theory for funnel dynamics will suffice for real proteins just as in the model systems. If the collective diffusion coefficients are wildly different for these extra degrees of freedom or when there is a free energy profile for the coupled order parameters with several minima, one must generalize the Kramer’s expression to a few more dimensions. We believe such a few-dimensional generalization of the current diffusive dynamical description should suffice for the smaller fast folding protein molecules. On the other hand, sufficiently

large proteins doubtless require a description in terms of geometrically localized order parameters not just a globally defined coordinate. One example of geometrically localized phenomena is provided by foldons.²² Foldons are kinetically autonomous folding subunits, that are expected to exist in the larger proteins. Each foldon will have its own funnel. A related description involving local collective coordinates necessary for describing critical nuclei may also be helpful. Some arguments suggest critical nuclei may be large²³ so the system would be well treated by global reaction coordinate while others suggest nuclei may small²⁴ or indeed possibly unique.²⁵ Any of these cases can be accommodated by the diffusive funnel dynamics picture once the coordinates are specified. We expect the diffusive funnel dynamics picture (discussed here and previously by us³) will provide a convenient quantitative framework to analyze both simulation and laboratory experiments.

-
1. P. E. Leopold, M. Montal, and J. N. Onuchic, *Proc. Natl. Acad. Sci. USA* **89**, 8721 (1992).
 2. J. D. Bryngelson, J. N. Onuchic, N. D. Socci, and P. G. Wolynes, *PROTEINS: Structure, Function and Genetics* **21**, 167 (1995).
 3. J. N. Onuchic, P. G. Wolynes, Z. Luthey-Schulten, and N. D. Socci, *Proc. Natl. Acad. Sci. USA* **92**, 3626 (1995).
 4. P. G. Wolynes, J. N. Onuchic, and D. Thirumalai, *Science* **267**, 1619 (1995).
 5. K. A. Dill, K. M. Fiebig, and H. S. Chan, *Proc. Natl. Acad. Sci. USA* **90**, 1942 (1993).
 6. K. A. Dill, S. Bromberg, K. Yue, K. M. Fiebig, D. P. Yee, P. D. Thomas, and H. S. Chan, *Protein Science* **4**, 561 (1995).
 7. E. M. Boczek and C. L. Brooks, *Science* **269**, 393 (1995).
 8. J. D. Bryngelson and P. G. Wolynes, *Proc. Natl. Acad. Sci. USA* **84**, 7524 (1987).
 9. J. D. Bryngelson and P. G. Wolynes, *J. Phys. C* **93**, 6902 (1989).
 10. N. D. Socci and J. N. Onuchic, *J. Chem. Phys.* **101**, 1519 (1994).
 11. N. D. Socci and J. N. Onuchic, *J. Chem. Phys.* **103**, 4732 (1995).
 12. R. Miller, C. A. Danko, M. J. Fasolka, A. C. Balazs, H. S. Chan, and K. A. Dill, *J. Chem. Phys.* **96**, 768 (1992).
 13. H. S. Chan and K. A. Dill, *J. Chem. Phys.* **99**, 2116 (1993).
 14. H. S. Chan and K. A. Dill, *J. Chem. Phys.* **100**, 9238 (1994).
 15. A. Šali, E. Shakhnovich, and M. Karplus, *J. Mol. Biol.* **235**, 1614 (1994).
 16. H. A. Kramers, *Physica* **7**, 284 (1940).

17. J. N. Onuchic and P. G. Wolynes, *J. Phys. Chem.* **92**, 6495 (1988).
18. V. B. P. Leite and J. N. Onuchic, preprint (1995).
19. R. F. Grote and J. T. Hynes, *J. Chem. Phys.* **73**, 2715 (1980).
20. A. Šali, E. Shakhnovich, and M. Karplus, *Nature* **369**, 248 (1994).
21. J. Wang and P. G. Wolynes, preprint (1995).
22. A. Panchenko, Z. Luthey-Schulten, and P. G. Wolynes, preprint (1995).
23. J. D. Bryngelson and P. G. Wolynes, *Biopolymers* **30**, 177 (1990).
24. Z. Y. Guo and D. Thirumalai, *Biopolymers* **36**, 83 (1995).
25. V. I. Abkevich, A. M. Gutin, and E. I. Shakhnovich, *Biochemistry* **33**, 10026 (1994).